IMAGING DIAGNOSIS—LEFT RETROCAVAL URETER AND TRANSPOSITION OF THE CAUDAL VENA CAVA IN A DOG

ANNE CAROLE DUCONSEILLE, ARNAUD LOUVET, PATRICK LAZARD, SUZY VALENTIN, MARC MOLHO

Retrocaval ureter and transposition of the caudal vena cava are each, rare developmental anomalies. We describe the usefulness of static fluid magnetic resonance urography and dynamic contrast-enhanced magnetic resonance urography in the diagnosis of these anomalies. Basic techniques, benefits, and drawbacks of magnetic resonance urography are presented. *Veterinary Radiology & Ultrasound, Vol. 51, No. 1, 2010, pp 52–56.*

Key words: abdomen, dog, hydronephrosis, MRI, vascular malformation.

Signalment, History, and Clinical Findings

AN 8-YEAR-OLD neutered female Bernese Mountain Dog was evaluated for chronic diarrhea. Two years previously the dog had been diagnosed histopathologically with moderate plasmocytic duodenitis. No physical abnormalities were detected. Hematologically, there was marked thrombocytosis (1,182,000/mm^3; reference range 250,000–550,000/mm^3). Bone marrow was characterized by reactive megakaryocytic hyperplasia, and a macrophagic hemosiderosis associated with atypic monocytes leading to a suspicion of hemophagocytic histiocytic sarcoma.

Imaging

Sonographically, the left renal pelvis was enlarged at 4 cm and there was marked ureteral dilation at 2 cm. A cause for the ureterohydronephrosis was not apparent. The right kidney appeared smaller than normal, was irregularly shaped and there was a loss of corticomedullary definition.

Magnetic resonance (MR) imaging was performed using a 1 T scanner.* Images were acquired with the following sequences: T1-weighted gradient-echo in dorsal and transverse planes, T2-weighted turbo spin-echo with and without fat saturation in dorsal and transverse planes. T1-weighted gradient-echo images in dorsal and transverse planes were repeated after intravenous injection of gadoteric acid.† To define the vascular abdominal anatomy and to follow the passage of contrast medium through both kidneys, dynamic contrast-enhanced MR urography was also performed. A three-dimensional (3D) T1-weighted gradient-echo fast low angle shot (FLASH) sequence was acquired in the dorsal plane. A precontrast mask was acquired, then a contrast medium detection sequence was performed‡ in the area of the abdominal aorta. The same dose of gadoteric acid was reinjected intravenously. When the contrast medium appeared in the cranial part of the abdominal aorta, acquisition of the 3D FLASH with elliptic centric view ordering of *k*-space was started. Three consecutive 3D volume acquisitions were repeated after 3, 5, and 10 min.

The marked pyelectasis and dilation of the proximal part of the left ureter were clearly seen. The left proximal ureter had a medial and dorsal deviation and the dilation ended abruptly in the area of a large, left sided curving abdominal vessel suspected to be a malpositioned caudal vena cava (Fig. 1). In the transverse plane, the end of the dilated part of the ureter was seen immediately dorsally to this large abdominal vessel. The left ureter was barely visible distal to the occlusion (Fig. 1B). The left ureter was occluded between the dorsal wall of the caudal vena cava and the ventral surface of the psoas muscles (Fig. 2). After the first contrast medium injection, the transposition of the caudal vena cava on the left side of the aorta was apparent. No enhancing lesion could be detected in the area of the left ureteral occlusion (Fig. 3). In the 3D FLASH mask sequence acquired 9 min after the first contrast medium injection, excretion of gadolinium into the left renal collecting system was evident, and the contrast medium had the same appearance as in the static T2-weighted dorsal images. Enhancement of the right renal collecting system was faintly visible in comparison to the left side. There were two renal arteries supplying each kidney. The arteriographic series eliminated the aorta as the cause of the left ureteral compression, and confirmed the left sided dis-

*Magnetom Harmony; Siemens, Erlangen, Germany.
†Dotarem, Guerbet, Roissy, France.
‡CareBolus, Siemens.

From the Centre d'Imagerie par Resonance Magnetique de l'Animal (Duconseille, Louvet), the Small Animal Veterinary Clinic (Louvet, Lazard, Valentin), 80 rue Pereire, 78 100 Saint Germain en Laye, France, and the Service de Radiologie, Centre Hospitalier Intercommunal, 78 300 Poissy-Saint Germain, France (Molho), .

Address correspondence and reprint requests to Arnaud Louvet, at the above address. E-mail: arnaud.louvet@ladelou.com

Received May 24, 2009; accepted for publication July 5, 2009.
doi: 10.1111/j.1740-8261.2009.01621.x

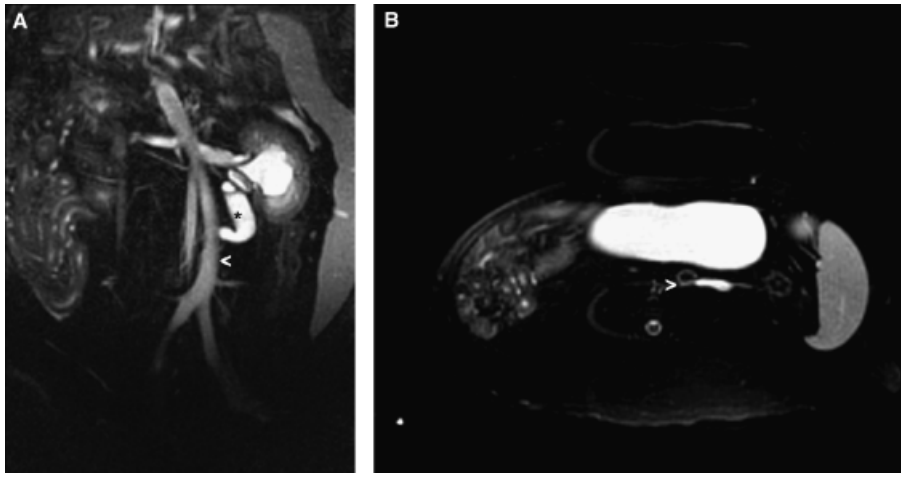

FIG. 1. (A) Static-fluid T2-weighted TSE fat-saturated dorsal image (TR = 5000 ms, TE = 97 ms). The marked pyelectasis and dilation of the proximal part of the left ureter are clearly seen (black star). The left proximal ureter is characterized by a medial and dorsal deviation and the dilation ends abruptly in the area of a large, left sided curving abdominal vessel suspected to be a malpositioned caudal vena cava (white arrowhead). Right is to the left and cranial is to the top. (B) In the transverse plane, the end of the dilated part of the left ureter is seen dorsal to this large abdominal vessel (arrowhead). The left ureter was barely visible distal to the occlusion. Right is to the left and ventral is to the top.

placement of the caudal vena cava. The vein crossed the midline of the abdomen near the aortic trifurcation where it curved laterally, crossed dorsal to it and then coursed laterally to the left side of the abdominal aorta to the ostia of the cranial renal arteries where it crossed ventrally. The dilated left ureter ended abruptly to the left of the caudal vena cava (Fig. 4). The final diagnosis was left ureterohydronephrosis secondary to transposition of the caudal vena cava and retrocaval ureter.

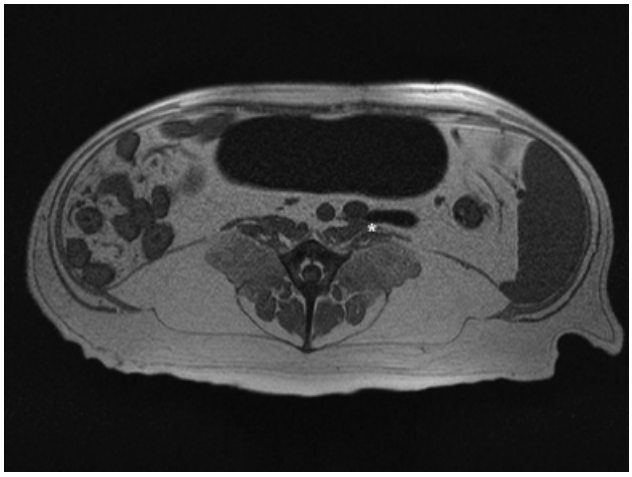

FIG. 2. T1-weighted transverse gradient-echo sequence (TR = 166 ms, TE = 7.49 ms, flip angle 70°) centered in the area of the ureteral dilation confirms the occlusion of the left ureter between the dorsal wall of the caudal vena cava and the ventral surface of the psoas muscles (white star). Right is to the left and ventral is to the top.

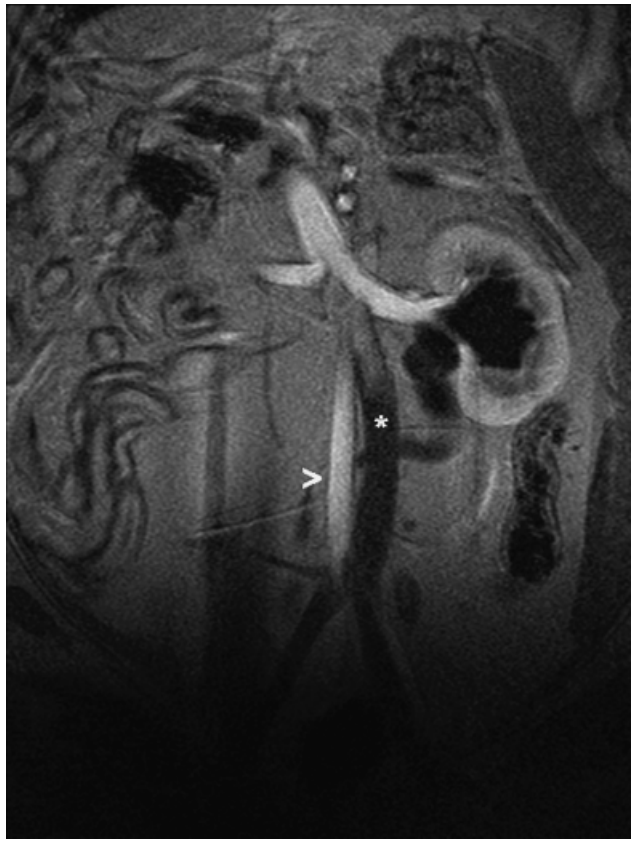

FIG. 3. T1-weighted dorsal gradient-echo sequence (TR = 148 ms, TE = 7.49 ms, flip angle 70°) acquired immediately after intravenous contrast medium injection confirms the transposition of the nonenhanced caudal vena cava (white star) on the left side of the opacified aorta (arrowhead). Right is to the left and cranial is to the top.

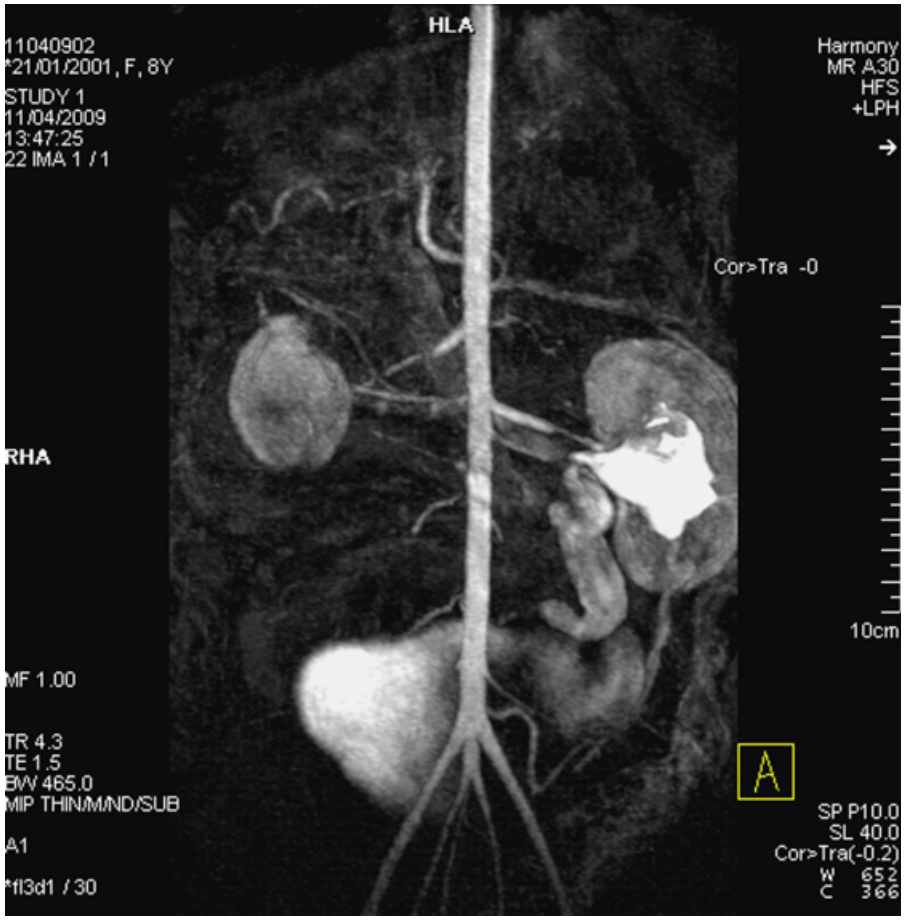

FIG. 4. Composite image of dorsal subvolume maximum intensity projection derived from the 3D T1-weighted (FLASH) sequence (TR = 4.3 ms, TE = 1.54 ms, flip angle 30°). This image excludes the aorta as the cause of the left ureteral compression. Opacification of the right renal collecting system was delayed in comparison to the left side. Right is to the left and cranial is to the top.

Discussion

In humans, the prevalence of transposition, or left sided inferior vena cava is 0.2–0.5%. Retrocaval ureter is a rare congenital anomaly resulting from the abnormal development of the inferior vena cava with a prevalence of 0.1%, with a two to threefold predominance in males. Only two human patients with both anomalies have been described.[1,2] A left-sided circumcaval ureter has been described in a young dog but no mention was made of transposition of the caudal vena cava.[3] A circumcaval ureter has been described in the cat.[4]

The embryogenesis of the caudal vena cava is complex, involving anastomosis and regression of three paired venous systems; the posterior cardinal, the subcardinal, and the supracardinal systems. This complex embryogenesis may result in four aberrant anatomic variants: duplicated caudal vena cava, transposition or left sided caudal vena cava, retroaortic left renal vein, and circumaortic left renal vein. Multiple concurrent vascular anomalies have occasionally been reported in humans[5] as well as in animals.[3] Concurrent congenital nonvascular abnormalities have also been reported frequently in humans with retrocaval ureter, including glandular hypospadia, supernumerary lumbar vertebra, syndactylia, and intestinal malrotation.[5] Development of the left sided caudal vena cava and retrocaval ureter as described in our dog requires two simultaneous caudal vena cava anomalies: the left sided caudal vena cava requires persistence of the left venous system that normally partially disappears and the formation of the retrocaval ureter requires persistence of the left subcardinal vein, which is ventral to the definitive ureteral position, rather than the left supracardinal vein as the renal segment of the caudal vena cava.[1]

Most often, retrocaval ureter is identified during the third or fourth decade of life, however, symptomatic pediatric patients have been described.[3,6] Gradual development of hydronephrosis accounts for the low incidence of detection during childhood.[6] In most patients, symptoms are related to ureteral obstruction and hydronephrosis. Pain can be intermittent and dull. Varying degrees of hematuria are noted in many patients.[7]

Diagnosis of retrocaval ureter is usually established by excretory urography and retrograde pyelography. But, when the diagnosis cannot be established with these methods, the combination of retrograde pyelography and cavography has been used. However, these procedures are invasive. Contrast-enhanced computed tomography and MR urography are the least invasive ways to diagnose retrocaval ureter. MR urography can be performed using unenhanced MR urography based on heavily T2-weighted pulse sequences, or gadolinium-enhanced MR urography.[8]

Static fluid MR urography can be used as an alternative to conventional excretory urography to obtain high-quality images of the dilated upper urinary tract and adjacent abnormalities. Static fluid MR urography does not require the excretion of contrast medium and is useful for evaluating the dilated collecting system of a poorly functional kidney.[9] Gadolinium-enhanced MR urography provides both functional information and detailed morphologic information concerning the ureters and periureteral tissue allowing a patient to be evaluated for the full spectrum of obstructive and nonobstructive ureteral diseases.[8,9] Unless used in patients with severe renal dysfunction where gadolinium contrast medium has been related to nephrogenic systemic fibrosis, gadolinium-enhanced MR imaging is considered safe and indicated in patients who cannot tolerate iodinated contrast medium and in patients with moderately reduced excretory function.[10]

A protocol for gadolinium-enhanced MR imaging has been described recently.[9] A 3D fat-suppressed echo-gradient sequence is acquired before and at times after contrast medium injection. By obtaining pre- and postcontrast images using identical imaging parameters, subtracted images that are particularly useful for the assessment of enhancing lesions can be obtained. After gadolinium-based contrast medium injection, magnetic resonance angiography (MRA) may be performed during the first pass of contrast medium through the aorta and renal arteries. Evaluation of the venous system is generally possible on subsequent images.[9,11–14] Excretory phase images of the contrast medium from the renal cortex to the ureters can usually be obtained approximately 5 min after gadolinium injection in humans. By combining various indices (differential renal function, renal transit time of contrast medium, peak relative signals in the cortex, medulla and calyces, washout rates, slope clearance of contrast medium) provided by gadolinium-enhanced MR urography, along with the anatomic information available from the same MR imaging examination, it is possible to provide an accurate diagnosis of obstruction and quantitatively evaluate quantitatively the ability of the cortex and medulla of each kidney to concentrate and excrete the contrast medium. Subtle changes of renal function can be analyzed.[13–15] Moreover, MRA has proved to be particularly useful in a large spectrum of nephrologic and urologic disease in humans, including the preoperative workup of kidney donors and evaluation of posttransplant renal failure in humans.[11] In our dog, the appearance of contrast medium in the right kidney was delayed compared with the left, as was the appearance of contrast medium in the right ureter. We therefore suspected a more advanced right renal dysfunction than in the obstructed left kidney.

Recently, analysis of data in humans obtained from dynamic MR urography has been shown to provide an accurate estimation of glomerular filtration rate. It is likely that in the near future, MR imaging will be able to provide similar information in comparison to renal scintigraphy.[13–15] The major drawbacks of MR urography are its high cost and its low sensitivity in the detection of calcifications when obstructive uropathy is suspected. However, the cost is offset by the fact that a single MR imaging examination provides anatomic information, and assessment of the vasculature and function of the kidneys.

Retrocaval ureter should be corrected surgically as soon as ureteral obstruction is present. This involves resection of the retrocaval segment and relocation of the anastomosis ventral to the caudal vena cava.[3,5] In our dog, functional information provided by gadolinium-enhanced MR urography suggested that a left nephrectomy should be avoided despite the ureteral obstruction. In this instance, our dog did not undergo surgery because of the high suspicion for histiocytic sarcoma.

In conclusion, although rare, retrocaval ureter should be considered in the differential diagnosis for ureterohydronephrosis. Gadolinium-enhanced MR urography offers a superb imaging technique to diagnose retrocaval ureter and provides functional information as well.

REFERENCES

1. Pierro JA, Soleimanpour M, Bory JL. Left retrocaval ureter associated with left inferior vena cava. Am J Roentgenol 1990;155:545–546.

2. Ishitoya S, Arai Y, Okubo K, et al. Left retrocaval ureter associated with the Goldenhar syndrome (brachial arch syndrome). J Urol 1997;158: 572–573.

3. Doust RT, Clarke S, Hammond G, Paterson C, King A. Circumcaval ureter associated with an intrahepatic portosystemic shunt in a dog. J Am Vet Med Assoc 2006;228:389–391.

4. Cornillie P, Baten T, Simoens P. Retrocaval ureter in a cat. Vet Rec 2006;159:24–25.

5. Rao J, Yang J, Liu Z, et al. Right retrocaval ureter and left nutcracker syndrome: a case report. Urology 2008;71:1226e9–1226e11.

6. Acharya SK, Jindal B, Yadav DK, Singha S, Bagga D. Retrocaval ureter: a rare cause of hydronephrosis in children. J Pediatr Surg 2009;44: 846–848.

7. Uthappa MC, Anthony D, Allen C. Case report—retrocaval ureter: MR appearances. Br J Radiol 2002;75:177–179.

8. Blandino A, Gaeta M, Minutoli F, et al. MR urography of the ureter. Am J Roentgenol 2002;179:1307–1314.

9. Leyendecker JR, Barnes CE, Zagoria RJ. MR urography: techniques and clinical applications. Radiographics 2008;28:23–46.

10. Kribben A, Witzke O, Hillen U, Barkhausen J, Daul AE, Erbel R. Nephrogenic systemic fibrosis. Pathogenesis, diagnosis, and therapy. J Am Coll Cardiol 2009;53:1621–1628.

11. Cerwinka WH, Grattan-Smith JD, Kirsch AJ. Magnetic resonance urography in pediatric urology. J Pediatr Urol 2008;4:74–83.

12. Cavrenne R, Mai W. Time-resolved contrast-enhanced MRA in normal dogs. Vet Radiol Ultrasound 2008;50:58–64.

13. Jones RA, Easley K, Little S, et al. Dynamic contrast-enhanced MR urography in the evaluation of pediatric hydronephrosis: part I, functional assessment. Am J Roentgenol 2005;185:1598–1607.

14. Jones RA, Perez-Brayfield MR, Kirsch AJ, Grattan-Smith JD. Renal transit time with MR urography in children. Radiology 2004;233: 41–50.

15. Boss A, Martirosian P, Gehrmann M, et al. Quantitative assessment of glomerular filtration rate with MR gadolinium slope clearance measurements: a phase I trial. Radiology 2007;243:783–790.